

Incoherent photon scattering by hydrogen forbidden in the dipole approximation

V. G. Gorshkov, A. I. Mikhailov, and S. G. Sherman

Leningrad Institute of Nuclear Physics, USSR Academy of Sciences

(Submitted January 28, 1974)

Zh. Eksp. Teor. Fiz. 66, 2020-2027 (June 1974)

Formulas are obtained for the cross section for the dipole-approximation-forbidden process of photon scattering by hydrogen atoms with electron transitions from the $1s$ to the $2p$ state. The formulas are valid in the entire nonrelativistic photon energy region where $\omega \ll m$, m being the electron mass.

1. INTRODUCTION

The cross sections for coherent and noncoherent scattering of photons by hydrogen atoms were recently obtained in analytic form with the aid of a closed expression for the Green function of an electron in the Coulomb field^[1-5]. In^[1-4] the authors use the dipole approximation: $\omega \sim I$, $\omega a \ll 1$, where I is the ionization potential and a is the Bohr radius. In^[6] it is shown that the formulas for the coherent and noncoherent scattering cross sections for any transitions between the atomic shells and for any values of ωa can be obtained without the use of the dipole approximation. These formulas take into account all orders of the power series expansion in the Coulomb parameter $\xi = (I/\omega)^{1/2}$, and go over, after being expanded in power series in the parameter ωa , into the formulas obtained in^[1-4] for $\xi \sim 1$ and $\omega a \ll 1$. In the region $\omega a \gtrsim 1$, $\xi \ll 1$, the formulas obtained in^[6] in the nonrelativistic approximation should be expanded in power series in the Coulomb parameter $\xi \ll 1$, since in this region the dominant contribution is made by the ξ -independent diagram for the direct transition (see Fig. 1a)^[7,8], while the ξ -dependent pole diagrams of Figs. 1b and 1c turn out to be of the order of the relativistic corrections even in terms of order ξ^0 . Therefore, the pole diagrams in the nonrelativistic approximation for $\omega a \gtrsim 1$ should be totally discarded (see^[7,8]).

Notice that for the incoherent processes that are allowed in the dipole approximation the contribution of the diagram for the direct transition is small when $\omega a \ll 1$ and $\xi \sim 1$. For these processes there exists, for $\xi \ll 1$ and $\omega a \ll 1$, a region where all the diagrams turn out to be of the same order of magnitude. This is discussed in detail at the end of the paper.

Using the formulas obtained in^[6], we can compute the cross sections for any processes forbidden in the dipole approximation. In this paper we obtain the cross section for the incoherent scattering connected with the $1s \rightarrow 2p$ transition of the hydrogen atom. This process is forbidden in the dipole approximation, and at photon energies of the order of the electron binding energy in the atom its cross section is $(\alpha Z)^{-2}$ times smaller than the cross section for the process involving the $1s \rightarrow 2s$ transition. At photon energies $\omega \sim \eta = m\alpha Z = 1/a$ the cross sections for the processes with the $1s \rightarrow 2p$ and $1s \rightarrow 2s$ transitions become, generally speaking, of the same order of magnitude. The $2p_{3/2}$ and $2s_{1/2}$ energy levels differ by the magnitude of the fine splitting, the $2p_{1/2}$ and $2s_{1/2}$ levels by the magnitude of the Lamb shift. Therefore, we shall compute the cross sections for the processes with transitions to the $2p_{3/2}$ and $2p_{1/2}$ levels separately.

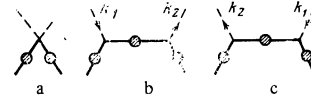


FIG. 1. Feynman diagrams for the process.

2. AMPLITUDE OF THE PROCESS

The wave function of an electron in the $2p_j$ state of the hydrogen atom has, in momentum space, the form

$$\langle f | \Psi_{jlm} \rangle = \left(\frac{4\pi}{3} \right)^{1/2} N_z \eta_z \left(-\frac{\partial}{\partial \eta_z} \right) \frac{8\pi f}{(f^2 + \eta_z^2)^2} \Omega_{jlm} \left(\frac{f}{f} \right), \quad (1)$$

where

$$N_z^2 = \eta_z^3 / \pi, \quad \eta_z = \eta / 2, \quad \eta = m\alpha Z, \quad (2)$$

$$\Omega_{jlm}(\mathbf{v}) = \begin{pmatrix} C_{m-\frac{1}{2}, \frac{1}{2}}^j Y_{l, m-\frac{1}{2}}(\mathbf{v}) \\ C_{m+\frac{1}{2}, -\frac{1}{2}}^j Y_{l, m+\frac{1}{2}}(\mathbf{v}) \end{pmatrix}.$$

Using the definition

$$Y_{lm}(\mathbf{v}) = \left(\frac{3}{4\pi} \right)^{1/2} \mathbf{e}_m \mathbf{v}, \quad \mathbf{e}_0 = \mathbf{e}_z, \quad \mathbf{e}_{\pm 1} = \mp \frac{1}{\sqrt{2}} (\mathbf{e}_x \pm i\mathbf{e}_y),$$

we obtain

$$\Omega_{jlm}(\mathbf{v}) = \left(\frac{3}{4\pi} \right)^{1/2} \begin{pmatrix} C_{m-\frac{1}{2}, \frac{1}{2}}^j \mathbf{e}_{m-\frac{1}{2}} \mathbf{v} \\ C_{m+\frac{1}{2}, -\frac{1}{2}}^j \mathbf{e}_{m+\frac{1}{2}} \mathbf{v} \end{pmatrix} = \Omega_{jlm} \mathbf{v}. \quad (3)$$

Using (3), we can rewrite (1) in terms of the derivatives of the Yukawa potential:

$$\langle f-k | \Psi_{jlm} \rangle = (4\pi/3)^{1/2} N_z \eta_z (\Omega_{jlm} \nabla_k) (-\partial/\partial \eta_z) \langle k | V_{in} | f \rangle, \quad (4)$$

where

$$\langle k | V_{in} | f \rangle = \frac{4\pi}{(f-k)^2 + \eta^2} = \langle f | V_{in} | k \rangle.$$

The wave function of the initial $1s$ state can similarly be written in the form

$$\langle f-k | \Psi_{10} \rangle = N_1 (-\partial/\partial \eta_1) \langle f | V_{in} | k \rangle \chi_{\mu}, \quad (5)$$

where χ_{μ} is the Pauli spinor.

The amplitude of the process is given by three Feynman diagrams in the Furry representation (see Fig. 1). The hatched blocks, which change the momenta, but not the energies, of the lines, represent the Coulomb wave functions and the Green function. The energy-momentum conservation law is satisfied at each vertex. The vertex of the diagram for the direct transition (Fig. 1a) is equal to the constant $4\pi\alpha(\mathbf{e}_2 \mathbf{e}_1)$, while the γ vertices in the diagrams in Figs. 1b and 1c have, in momentum space, the following form:*

$$\langle f | \gamma | f' \rangle = \frac{\sqrt{4\pi\alpha}}{m} \mathbf{e} \left(\mathbf{f} + \frac{i}{2} [\sigma \mathbf{k}] \right) \langle f-k | f' \rangle,$$

where \mathbf{e} and \mathbf{k} are respectively the polarization and momentum of the photon.

Using the expressions for the wave functions (4) and (5), we can easily verify that the action of the operator $-\mathbf{f}\partial/\partial\eta$ on (4) or (5) is equivalent to that of the operator $\eta\nabla_{\mathbf{k}}$. Taking the foregoing into account, we can represent the amplitude of the photon scattering by hydrogen with the $1s \rightarrow 2p$ transition for $\omega \ll m$ in the form (see^[6])

$$A_{j\mu} = 4r_0 \eta_2^{1/2} \eta_1^{1/2} \left(\frac{4\pi}{3}\right)^{1/2} (\Omega_{jm} \cdot \nabla_2) \left\{ (\mathbf{e}_2 \mathbf{e}_1) \frac{\lambda}{(q^2 + \lambda^2)^2} + \mathbf{e}_2 \left(2\eta_2 \nabla_2 + i[\sigma \mathbf{k}_1'] \frac{\partial}{\partial \eta_2} \right) \mathbf{e}_1 \left(2\eta_1 \nabla_1 - i[\sigma \mathbf{k}_1] \frac{\partial}{\partial \eta_1} \right) J(p) \right\} \chi_{\mu} \quad (6)$$

$$+ \left(\begin{array}{c} \mathbf{e}_2 \neq \mathbf{e}_1 \\ \mathbf{k}_2, \omega_2 \neq -\mathbf{k}_1, -\omega_1 \end{array} \right),$$

where

$$J(p) = \frac{\pi^2}{2m} \langle \mathbf{k}_2 | V_{im} G_c V_{im} | \mathbf{k}_1 \rangle = \frac{i}{p^3} \int_1^{\infty} \frac{t^{i\lambda} dt}{at^2 - 2bt + \bar{a}},$$

$$\lambda = \eta_1 + \eta_2, \quad a = a_1 a_2, \quad \bar{a} = \bar{a}_1 \bar{a}_2, \quad b = b_1 b_2 - 4n_1 n_2,$$

$$a_1 = n_1^2 - (1 + i\mu_1)^2, \quad \bar{a}_1 = n_1^2 - (1 - i\mu_1)^2, \quad b_1 = 1 + n_1^2 + \mu_1^2,$$

$$n_l = \frac{k_l}{p}, \quad \mu_l = \frac{\eta_l}{p}, \quad \nabla_l = \nabla_{\mathbf{k}_l} \quad (l=1,2), \quad (7)$$

$$\eta_1 = \eta = m\alpha Z, \quad \eta_2 = \eta/2, \quad \mathbf{q} = \mathbf{k}_1 - \mathbf{k}_2, \quad p = [2m(\omega_1 - \epsilon_1) + i0]^{1/2},$$

$$\omega_1 - \epsilon_1 = \omega_2 - \epsilon_2, \quad \epsilon_1 = \frac{\eta^2}{2m}, \quad \epsilon_2 = \frac{\eta^2}{8m},$$

$$\xi = \frac{\eta}{p}, \quad r_0 = \frac{\alpha}{m}, \quad \alpha = \frac{1}{137}.$$

Here $\mathbf{e}_1, \mathbf{k}_1, \omega_1$ and $\mathbf{e}_2, \mathbf{k}_2, \omega_2$ are the polarization, momentum, and energy of the initial and final photons; ϵ_1 and ϵ_2 are the binding energies of the initial and final electrons. The prime on \mathbf{k}_2 indicates that the gradient operator does not act on \mathbf{k}_2' .

3. PHOTON SCATTERING IN THE CASE WHEN $\omega \sim 1$

Computing the derivatives, and discarding the quantities $n_l^2 \sim \alpha^2 Z^2$ in comparison with unity, we obtain in the dipole region $\omega \sim 1 = \eta^2/2m$ the expressions

$$A_{j\mu} = N (\Omega_{jm} \cdot \xi \chi_{\mu}), \quad N = 2\sqrt{2} r_0 \eta^4 (4\pi/3)^{1/2};$$

$$\xi = \mathbf{v}_2 (\mathbf{e}_2 \mathbf{e}_1) L_1 + \mathbf{e}_2 (\mathbf{e}_1 \mathbf{v}_2) L_2 + \mathbf{e}_2 i[\sigma \mathbf{s}_1] L_3 + (\mathbf{e}_2, \mathbf{v}_2, \omega_2 \neq \mathbf{e}_1, \mathbf{v}_1, -\omega_1),$$

$$\mathbf{v}_l = \mathbf{k}_l / \omega_l, \quad \mathbf{s}_l = [\mathbf{e}_l \mathbf{v}_l], \quad L_1 = A_1 + B_2 + B_3, \quad L_2 = A_1 + B_2, \quad L_3 = A_3 + B_4; \quad (8a)$$

$$A_1 = -16i \frac{\omega_2}{p} [(1+i\xi)^2 J_2 + 2(1+\xi^2) J_2 + (1-i\xi)^2 J_1],$$

$$A_2 = 64i \frac{\omega_1}{p} J_3,$$

$$A_3 = \frac{\omega_1}{\eta} \left[(1+i\xi)^2 \left(1 + \frac{i\xi}{2} \right)^2 J_1 + (1+i\xi)^2 (2+i\xi) \left(3 + \frac{i\xi}{2} + \xi^2 \right) J_1 + 2i\xi (1+\xi^2) \left(4 + \frac{3}{4} \xi^2 \right) J_2 - (1-i\xi)^2 (2-i\xi) \left(3 - \frac{i\xi}{2} + \xi^2 \right) J_1 - (1-i\xi)^2 \left(1 - \frac{i\xi}{2} \right)^2 J_0 \right], \quad (8b)$$

$$A_4 = 16 \frac{\omega_2}{\eta} \left[\left(1 + \frac{i\xi}{2} \right) (1+i\xi)^2 J_2 + i\xi (1+\xi^2) J_1 - \left(1 - \frac{i\xi}{2} \right) (1-i\xi)^2 J_1 \right],$$

$$A_5 = 2(\nu_2)^2 \omega_1 / \eta, \quad B_l = A_l(\omega_1 \neq -\omega_2),$$

$$J_n = \frac{\xi^n}{a^3} \int_1^{\infty} \frac{t^{i\lambda+n} dt}{(t-x)^6} = \frac{\xi^n}{a^3} \frac{1}{5-n-i\xi^2} F_1(6, 5-n-i\xi, 6-n-i\xi, x) \quad (8c)$$

$$a = (1+i\xi)^2 \left(1 + \frac{i\xi}{2} \right)^2, \quad x = \frac{(1-i\xi)(2-i\xi)}{(1+i\xi)(2+i\xi)}, \quad \xi = \frac{\eta}{p}.$$

Using the definition (3) for the unit vectors ν and \mathbf{e} and the formula

$$\sum_{\mu} \Omega_{j\mu}(\mathbf{a}) \Omega_{j\mu}(\mathbf{b}) = \frac{1}{4\pi} \left\{ \left(j + \frac{1}{2} \right) (\mathbf{ba}) + (-1)^{j+1/2} i (\sigma[\mathbf{ba}]) \right\}, \quad (9)$$

we obtain the following expression for the cross section summed over the electron polarizations:

$$d\sigma_j(\mathbf{e}_2, \mathbf{e}_1) = \frac{1}{2} \sum_{\mu\mu'} |A_{j\mu\mu'}|^2 \frac{\omega_2}{\omega_1} d\Omega$$

$$= \frac{N^2}{4\pi} \left\{ \left(j + \frac{1}{2} \right) [(\mathbf{e}_2 \mathbf{e}_1)^2 (|L_1|^2 + \mathbf{v}_2 \mathbf{v}_1 \cdot \text{Re } L_1^* M_1) + (\mathbf{e}_2 \mathbf{v}_2)^2 |L_2|^2 + |L_3|^2 + (\mathbf{e}_2 \mathbf{e}_1) (\mathbf{e}_2 \mathbf{v}_1) (\mathbf{e}_1 \mathbf{v}_2) \text{Re } (L_2^* M_2 + 2L_1^* M_2) + (\mathbf{e}_2 \mathbf{e}_1) (\mathbf{s}_2 \mathbf{s}_1) \text{Re } L_3^* M_3] \right. \quad (10)$$

$$+ (-1)^{j+1/2} [-(\mathbf{e}_2 \mathbf{s}_1) (\mathbf{e}_1 \mathbf{s}_2) \text{Re } L_3^* M_3 - 2(\mathbf{e}_2 \mathbf{e}_1) (\mathbf{s}_2 \mathbf{s}_1) \text{Re } L_1^* L_3 - 2(\mathbf{e}_2 \mathbf{e}_1)^2 \text{Re } L_1^* M_3 + 2(\mathbf{e}_1 \mathbf{v}_2)^2 \text{Re } L_2^* M_3] + (\mathbf{e}_1, \mathbf{v}_1, \omega_1 \neq \mathbf{e}_2, \mathbf{v}_2, -\omega_2) \left. \right\} \frac{\omega_2}{\omega_1} d\Omega.$$

Averaging over the photon polarizations, and integrating over the angles, we obtain the following expressions for the differential and total cross sections:

$$\frac{d\sigma_j}{d\Omega} = \frac{1}{2} \sum_{\mathbf{e}_2, \mathbf{e}_1} \frac{1}{2} \sum_{\mu\mu'} |A_{j\mu\mu'}|^2 \frac{\omega_2}{\omega_1} = \frac{8}{3} r_0^2 \frac{\omega_2}{\omega_1} \left\{ \left(j + \frac{1}{2} \right) \left[\frac{1}{2} (1 + \cos^2 \theta) |L_1|^2 + \sin^2 \theta |L_2|^2 + 2|L_3|^2 + \frac{1}{2} (1 + \cos^2 \theta) \cos \theta \text{Re } (L_1^* M_1) - \frac{1}{2} \cos \theta \sin^2 \theta \text{Re } (L_2^* M_2 + 2L_1^* M_2) + \cos \theta \text{Re } (L_3^* M_3) + (-1)^{j+1/2} [\cos \theta \text{Re } (L_2^* M_3 - 2L_1^* L_3) - (1 + \cos^2 \theta) \text{Re } (L_1^* M_3) + 2 \sin^2 \theta \text{Re } L_2^* M_3] + (L_1^* M_1) \right] \right\}, \quad (11)$$

$$\sigma_j = \frac{8}{3} \sigma_0 \frac{\omega_2}{\omega_1} \left\{ \left(j + \frac{1}{2} \right) (|L_1|^2 + |L_2|^2 + 3|L_3|^2) + (-1)^{j+1/2} 2 \text{Re } (L_2^* M_3 - L_1^* M_3) + (L_1^* M_1) \right\}, \quad (12)$$

$$\sigma_0 = \frac{8}{3} \pi r_0^2, \quad r_0^2 = 7.95 \cdot 10^{-26} \text{ cm}^2, \quad \cos \theta = \mathbf{v}_2 \mathbf{v}_1, \quad (13)$$

$$M_l = L_l(\omega_1 \neq -\omega_2).$$

The differential and total cross sections for scattering with transitions to the entire 2p shell are determined by the sums of the cross sections (11) and (12) for $j = 1/2$ and $j = 3/2$,

4. PHOTON SCATTERING AT ENERGIES $1 \ll \omega \ll m$

In the energy region $\eta^2/2m \ll \omega \ll m$, the formula (6) can be expanded in a power series in the Coulomb parameter $\xi = (\eta^2/2m\omega)^{1/2} \ll 1$, which is equivalent to the replacement of the Green function of the intermediate electron in the Coulomb field by the Green function of the free electron. As a result, the process will be described by three nonrelativistic Born diagrams^[2,3] with amplitude

$$A_{1 \rightarrow 2p} = 4\sqrt{2} r_0 \frac{\eta^4}{(q^2 + \lambda^2)^2} \chi_2 \left\{ \frac{\lambda(\mathbf{e}\mathbf{q})(\mathbf{e}_2 \mathbf{e}_1)}{q^2 + \lambda^2} + \frac{i\lambda}{8m} [(\mathbf{e}\mathbf{e}_1)(\sigma[\mathbf{e}_2 \mathbf{v}_2]) + (\mathbf{e}\mathbf{e}_2)(\sigma[\mathbf{e}_1 \mathbf{v}_1])] \right\} \chi_1, \quad (14)$$

where $\lambda = \eta_1 + \eta_2 = 3/2 \eta$, $\mathbf{q} = \mathbf{k}_1 - \mathbf{k}_2$. The first term in (14) arises from the diagram for the direct transition (the first term in (6)), the last two from the pole diagrams (the last two terms in (6) for $\xi = 0$)^[5]. At large $q \sim \omega$ the dominant term in (14) is the first term, being greater by a factor of $m/q \sim m/\omega$ than the remaining two terms, which should be discarded, for the neglected relativistic corrections have the same order of magnitude^[1]. At small $q \sim \eta^2/2m$, the first term becomes equal in order of magnitude to the second term, and therefore to obtain the cross section for $q \sim \eta^2/2m$ it is necessary to carry out relativistic calculations.

After the neglect of the pole diagrams, the amplitude (14) ceases to depend on the spin, and, consequently, the cross sections for scattering with transitions to the $2p_{1/2}$ and $2p_{3/2}$ levels will differ in their statistical weights, which are respectively equal to $1/3$ and $2/3$.

Therefore, in the region $\eta^2/2m \ll \omega \ll m$ under consideration we shall only give the total cross section for the whole 2p shell:

$$\frac{d\sigma_{1s \rightarrow 2p}}{d\Omega} = 36r_0^2 \frac{\eta^{10} q^2}{(q^2 + \lambda^2)^6} (1 + \cos^2 \theta),$$

$$q \gg q_{\min} = \omega_1 - \omega_2 = \varepsilon_1 - \varepsilon_2 = \frac{3}{8} \frac{\eta^2}{m}. \quad (15)$$

The total cross section is ($q \sim q_{\min}$ make no contribution to the total cross section)

$$\sigma_{1s \rightarrow 2p} = \sigma_0 \left(\frac{2}{3} \right)^4 \frac{4\beta(20 + 16\beta + 11\beta^2 + 3\beta^3)}{5(1 + \beta)^2},$$

$$\beta = \frac{4\omega^2}{\lambda^2} = \left(\frac{4}{3} \frac{\omega}{\eta} \right)^2, \quad \omega_1 \approx \omega_2 = \omega. \quad (16)$$

The formulas (11) and (12) are respectively joined onto the formulas (15) and (16) in the region $\eta^2/2m \ll \omega \ll \eta$.

Let us also give, for comparison, the differential and total cross sections for the processes of photon scattering by the hydrogen atom with $1s \rightarrow 1s$ and $1s \rightarrow 2s$ transitions. The scattering with the $1s \rightarrow 1s$ transition in the photon-energy region $\eta^2/2m \ll \omega \ll m$ is determined by only the direct-transition diagram^[7], and has the form

$$\frac{d\sigma_{1s \rightarrow 1s}}{d\Omega} = \frac{r_0^2}{2} \left(\frac{4\eta^2}{q^2 + 4\eta^2} \right)^4 (1 + \cos^2 \theta), \quad (17)$$

$$\sigma_{1s \rightarrow 1s} = \sigma_0 \frac{2 + 2\beta_0 + \beta_0^2}{2(1 + \beta_0)^3}, \quad \beta_0 = \left(\frac{\omega}{\eta} \right)^2. \quad (18)$$

The amplitude of the scattering with the transition to the 2s state in the region $I \ll \omega \ll \eta$ is determined by the sum of all the three diagrams in Fig. 1:

$$A_{1s \rightarrow 2s} = 4\sqrt{2} r_0 (\mathbf{e}_1 \mathbf{e}_2) \left\{ \frac{\eta^4 q^2}{(q^2 + \lambda^2)^3} + \frac{1}{3} \left(\frac{I}{\omega} \right)^2 \left[1 + O \left(\frac{I}{\omega} \right) \right] \right\}, \quad I = \frac{\eta^2}{2m}. \quad (19)$$

The cross section for scattering accompanied by the transition of the atom to the 2s state has the form

$$\frac{d\sigma_{1s \rightarrow 2s}}{d\Omega} = \frac{1}{2} \sum_{\mathbf{e}_1, \mathbf{e}_2} |A|^2 \frac{\omega_2}{\omega_1}$$

$$= 16r_0^2 (1 + \cos^2 \theta) \left\{ \frac{\eta^8 q^4}{(q^2 + \lambda^2)^6} + \frac{2}{3} \frac{\eta^4 q^2}{(q^2 + \lambda^2)^3} \left(\frac{I}{\omega} \right)^2 + \frac{1}{9} \left(\frac{I}{\omega} \right)^4 \right\}, \quad (20)$$

$$\sigma_{1s \rightarrow 2s} = \frac{32}{9} \sigma_0 \left\{ \frac{\beta^2 (7 + 2\beta + \beta^2)}{5(1 + \beta)^5} \left(\frac{2}{3} \right)^6 + \frac{2}{\beta^2} \left(\frac{12 + 22\beta + 10\beta^2 + \beta^3}{(1 + \beta)^2} \right) \right.$$

$$\left. - \frac{12 + 4\beta}{\beta} \ln(1 + \beta) \right\} \left(\frac{2}{3} \frac{I}{\omega} \right)^2 + \left(\frac{I}{\omega} \right)^4, \quad \beta = \left(\frac{4}{3} \frac{\omega}{\eta} \right)^2. \quad (21)$$

The amplitudes of the $1s \rightarrow ns$ processes have, in the zeroth approximation in the parameter ω_1/m , the following form:

$$A(q^2, \omega_1) = f_0(q^2) + \left(\frac{I}{\omega_1} \right)^2 f_2(q^2) + O \left(\frac{I^3}{\omega_1^3} \right).$$

There is no linear term in the power series expansion in the parameter I/ω_1 on account of the invariance of the amplitude under the substitution $\omega_1 \rightleftharpoons -\omega_2 \approx -\omega_1$. For $\omega \gtrsim \eta$, only the first terms, which are determined by the diagram in Fig. 1a, remain in (20) and (21). For $\omega \ll \eta(\alpha Z)^{1/2}$, the last term (given by the diagrams of Figs. 1b and 1c) in each expression becomes the dominant term. The matching of the formulas (20) and (21) with the results obtained in^[2] occurs in the region $I \ll \alpha \ll \eta(\alpha Z)^{1/2}$.

The inelastic-scattering cross sections (16), (18), and (21) peak in the region $\omega \sim \eta$. In this region the cross sections for scattering with the transition of an electron to an excited level coincide in order of magnitude with

the elastic cross section and with the cross section for scattering accompanied by the ionization of the atom. This is connected with the fact that for $\omega \sim \eta$ the phase volumes of the electrons in the continuous and discrete spectra are of the same order of magnitude $d^3p \sim \eta^3$. The sum of all the cross sections for scattering with transitions to arbitrary shells, including the ground state and the continuum, each of which is determined by a direct-transition diagram, is, for $\omega \sim \eta$, equal to the classical Thomson cross section σ_0 ^[7]. This sum rule follows from the completeness condition for the electron wave functions, if we take into account the fact that the dominant contribution to the integral over the continuous spectrum under the completeness condition is made by the final-electron momenta $p \sim \eta$, whereas the kinematic limit $p_{\max} = \sqrt{2m\omega} \gg \eta$ ^[8].

As $\omega > \eta$ increases, the cross sections for scattering with transitions to discrete final levels, while remaining equal in order of magnitude, decrease: $\sigma_{1s \rightarrow n} \sim \sigma_0 \eta^2 / \omega^2$ (see (16), (18), and (21)). This is a consequence of the concentration of these processes in the region of small angles: $q \sim \eta$ or $\theta \sim \eta/\omega$. In this region the dominant process is the one accompanied by the ionization of the atom, the cross section for this process being equal to σ_0 for $\eta \ll \omega \ll m$.

For small ω in the region $I \ll \omega \ll \eta$ all the inelastic-scattering cross sections, including the total cross section for scattering with ionization, decrease in magnitude, while the elastic cross section (18) becomes equal to σ_0 . As a result, the sum of the cross sections for elastic and inelastic scattering, including the processes with ionization, is equal to σ_0 in the entire region $m \gg \omega \gg I$. The decrease in magnitude of (16) and (21) with decreasing ω is connected with the fact that the orthogonality of the wave functions for off-diagonal transitions leads to the vanishing of the direct-transition diagrams at $q=0$. In this case for the processes forbidden in the dipole approximation the vanishing of the amplitude is linear with respect to q (there is also the vector \mathbf{e} ; see (14)), while for the allowed processes it is quadratic. Accordingly, the cross sections (16) and (21) decrease in proportion to $\sigma_0 \omega^2 / \eta^2$ and $\sigma_0 \omega^4 / \eta^4$. Therefore, for $\eta \gg \omega \gg \eta(\alpha Z)^{1/2}$, the cross section (16) parametrically exceeds the cross section (21). The decrease of the cross sections (16) and (21) will continue until the pole diagrams of Figs. 1b and 1c become equal in order of magnitude to the direct-transition diagram. The contribution to the cross section of the pole diagrams for the processes allowed in the dipole approximation increases in magnitude with decreasing ω according to the law $\sigma_0(\eta^2/2m\omega)^4$, whereas for the forbidden transitions it remains a constant $\approx \sigma_0 \eta^2 / m^2 = (\alpha Z)^2 \sigma_0$. The cross section (16) will exceed the cross section (21) until the pole diagrams $\sim r_0(\eta^2/2m\omega)^2$ exceed the value ($\sim r_0\omega/\eta$) of the direct-transition diagram in (16), i.e., as long as $\omega \gg \eta(\alpha Z)^{2/3}$. In this connection, the formula (21), which includes the pole diagrams, has a minimum at $\omega \sim \eta(\alpha Z)^{1/2}$. On the other hand, the cross section (16) decreases right up to values of the order of $\sigma_0(\alpha Z)^2$ when $\omega \sim I$, and the formula (16), which is determined only by the direct-transition diagram in Fig. 1a, remains valid everywhere when $\omega \gg I$.

The entire analysis carried out in the present paper is based on the smallness of the parameter $\alpha Z \ll 1$. When $\alpha Z \sim 1$, a relativistic treatment of the problem with the Dirac wave functions and the Green functions

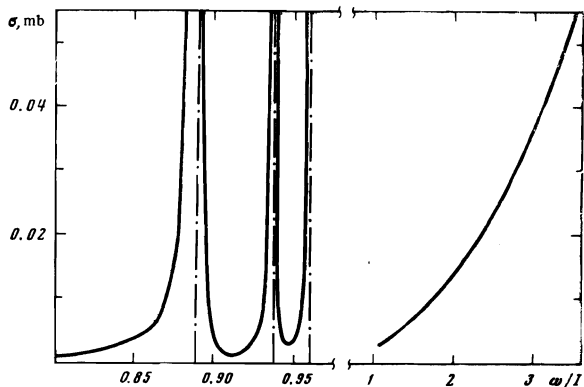


FIG. 2. Total cross section for photon scattering by hydrogen accompanied by the transition of the atom from the $1s$ to the $2p_{3/2}$ state for photon energies of the order of the ionization potential.

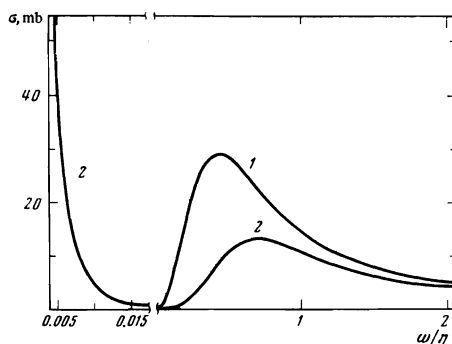


FIG. 3. Total cross section for photon scattering by hydrogen accompanied by the $1s \rightarrow 2p_{3/2}$ transition (curve 1) and by the $1s \rightarrow 2s$ transition (curve 2) for $\omega \gg I$.

of an electron in the Coulomb field of the atom is necessary for any ω (see, for example, ^[9]).

Figures 2 and 3 show the behavior of the total cross section for light scattering by the hydrogen atom with a transition from the $1s$ to the $2p_{3/2}$ state as a function of the photon energy when $\omega \sim I$ (Fig. 2) and $\omega \gg I$ (Fig. 3).

For the case when the final state is the $2p_{1/2}$ state the cross section is smaller by a factor of two, since the second term in (12) is small almost everywhere except in small regions in the vicinities of resonances. Figure 3 also shows a plot of the cross section for scattering accompanied by the $1s \rightarrow 2s$ transition. The part of this graph with $\omega \ll \eta(\alpha Z)^{1/2}$ was plotted using the results of the paper ^[2], while the part for large ω was plotted using the formula (21).

The authors are grateful to E. Drukarev, V. Polikanov, and A. Shelankov for their help in the computations and for discussions.

* $[\sigma k] \equiv \sigma \times k$.

¹⁾The relativistic corrections are smaller in magnitude than the first term in (6) by a factor of $v^2 = p^2/m^2 = 2m\omega/m^2 \sim \omega/m$ ^[5].

¹⁾M. Gavril, Phys. Rev. **163**, 147 (1967).

²⁾B. A. Zon, N. L. Manakov, and L. P. Rapoport, Zh. Eksp. Teor. Fiz. **55**, 924 (1968) [Sov. Phys.-JETP **28**, 480 (1969)].

³⁾S. I. Vetchinkin and S. V. Khristenko, Opt. Spektrosk. **25**, 650 (1968) [Opt. Spectrosc. **25**, 365 (1968)].

⁴⁾Ya. I. Granovskii, Zh. Eksp. Teor. Fiz. **56**, 605 (1969) [Sov. Phys.-JETP **29**, 333 (1969)].

⁵⁾V. G. Gorshkov, A. I. Mikhailov, V. S. Polikanov, and S. G. Sherman, Phys. Lett. **A30**, 455 (1969).

⁶⁾V. G. Gorshkov and V. S. Polikanov, ZhETF Pis. Red. **9**, 464 (1969) [JETP Lett. **9**, 279 (1969)].

⁷⁾G. Wentzel, Z. Phys. **43**, 779 (1927); **58**, 348 (1929).

⁸⁾A. Sommerfeld, Atomic Structure and Spectral Lines, Vol. 2, Methuen & Co. Ltd., London, 1934 (Russ. Transl., Gostekhizdat, 1956, p. 507).

⁹⁾I. B. Whittingham, J. Phys. **A4**, 21 (1971).

Translated by A. K. Agyei